J. Microbiol. Biotechnol. (2011), **21**(2), 162–169
doi: 10.4014/jmb.1007.07066
First published online 19 November 2010

JOURNAL OF MICROBIOLOGY AND BIOTECHNOLOGY

Dynamic Modeling of Lactic Acid Fermentation Metabolism with *Lactococcus lactis*

Oh, Euhlim[1], Mingshou Lu[1], Woo Joo Choi[1], Changhun Park[2,3], Han Bin Oh[2], Sang Yup Lee[4], and Jinwon Lee[1]*

[1]*Department of Chemical and Biomolecular Engineering, Sogang University, Seoul 121-742, Korea*
[2]*Department of Chemistry, Sogang University, Seoul 121-742, Korea*
[3]*Clinical Trials Center, Yonsei University Health System, Seoul 120-725, Korea*
[4]*Department of Chemical and Biomolecular Engineering, Korea Advanced Institute of Science and Technology, Daejeon 305-701, Korea*

Received: July 30, 2010 / Accepted: November 1, 2010

A dynamic model of lactic acid fermentation using *Lactococcus lactis* was constructed, and a metabolic flux analysis (MFA) and metabolic control analysis (MCA) were performed to reveal an intensive metabolic understanding of lactic acid bacteria (LAB). The parameter estimation was conducted with COPASI software to construct a more accurate metabolic model. The experimental data used in the parameter estimation were obtained from an LC–MS/MS analysis and time-course simulation study. The MFA results were a reasonable explanation of the experimental data. Through the parameter estimation, the metabolic system of lactic acid bacteria can be thoroughly understood through comparisons with the original parameters. The coefficients derived from the MCA indicated that the reaction rate of L-lactate dehydrogenase was activated by fructose 1,6-bisphosphate and pyruvate, and pyruvate appeared to be a stronger activator of L-lactate dehydrogenase than fructose 1,6-bisphosphate. Additionally, pyruvate acted as an inhibitor to pyruvate kinase and the phosphotransferase system. Glucose 6-phosphate and phosphoenolpyruvate showed activation effects on pyruvate kinase. Hexose transporter was the strongest effector on the flux through L-lactate dehydrogenase. The concentration control coefficient (CCC) showed similar results to the flux control coefficient (FCC).

Keyword: Lactic acid, chemostat, intracellular metabolite flux analysis, parameter estimation, metabolic control analysis, LC–MS

Conventionally, lactic acid has generated interest as a food additive, a component of health care supplies, and a preservative [26]. However, in recent years, lactic acid generates interest as a substitution material of polymers [3]. PLA (polylactic acid) is one of the famous examples of a biodegradable polymer. Moreover, with the greenhouse effect becoming more serious, recent research is mainly focused on replacing the traditional oil industry with green and clean bioindustries. In the same context, the lactic acid fermentation process is being highly studied. If biotechnology-produced PLA can become an alternate material of fossil fuel-based chemicals, the amount of CO_2 emissions can be significantly reduced to step towards the goal of sustainable development. For these kinds of studies, systems biotechnology is an essential tool for the prediction and analysis of the fermentation mechanisms of lactic acid metabolism.

Systems biotechnology is based on high-throughput experimental instruments, which can produce enormous amount of omics data. In systems biotechnology, the computational modeling of metabolism, based on quantitative data of cellular metabolites and specific mathematical equations, can suggest predictive results of experiments or novel approaches to perform better experiments [12].

Although there were several attempts to construct a kinetic model of lactic acid bacteria [11, 14], most of these models are extremely simplified or targeted for other products. Additionally, almost none of them included parameter estimation and a control analysis based on experimental data with a detailed pathway model. In this study, a full kinetic model of glycolysis in *Lactococcus lactis* subsp. *lactis* (ATCC 19435) was constructed. Enzyme kinetic parameters were estimated from *in vivo* intracellular metabolite concentrations to construct a more accurate kinetic model. Both metabolic flux analysis (MFA) and metabolic control analysis (MCA) were performed for every considered enzyme and metabolite. MATLAB COPASI and Mathmatica software were used for the calculation and

**Corresponding author*
Phone: +82-2-705-8919; Fax: +82-2-702-7926;
E-mail: jinwonlee@sogang.ac.kr

simulation of the kinetic metabolism of the lactic acid bacteria *Lactococcus lactis* subsp. *lactis*.

Materials and Methods

Organisms and Growth Media

Lactococcus lactis subsp. *lactis* (ATCC 19435) was obtained from the Korean Collection for Type Cultures (KCTC). For the pre-culture of the strain, commercial MRS broth (Difco, USA) was used. For all other fermentation steps, the growth medium composition was adopted from semidefined media proposed by van Niel *et al*. [25], except for glucose. The glucose concentration was reduced to 5 g/l for the establishment of a glucose-limited chemostat culture condition. Every instrument and growth medium was autoclaved at 121°C for 15 min. Deionized water (DW) was obtained using a water purification system (Human Power I$^+$, Human Corporation, Korea).

Culture Method and Growth Conditions

A single glycerol stock was inoculated into 100 ml of MRS broth and cultured for 15 h in a shaking incubator (SI-600R; Jeiotech, Korea). The culture condition was 33.5°C at 200 rpm, and the cell growth was monitored with the optical density at 600 nm (OD_{600}) using a UV–Vis spectrophotometer (BioSpec-mini; SHIMADZU, Japan). When the optical density reached around 1.2, 100 ml of culture broth was centrifuged using a table-top centrifuge (VS-550N; Vision Scientific Co., Ltd, Korea) for 10 min at 4,500 rpm. Cells were washed once and inoculated into 1 l of defined medium. The temperature and agitation speed were the same as the preculture step. The pH was maintained at a constant value of 6.0 with 2.5 N NaOH solutions. Fermentation was performed in a 5-l fermenter (Li-Flux GX; Biotron, Korea) controlled automatically with a connected controller.

The chemostat culture was started at the glucose exhaustion point with a dilution ratio of 0.2 h^{-1} using a periplastic pump (MasterFlex L/S, Cole-Parmer Instrument Company, USA) and silicon tube (MasterFlex, Cole-Parmer Instrument Company, USA). The steady-state was established after flushing the working volume five times.

During the whole process, 4 ml of sample was taken every 2 h. Then 2 ml of sample was used for the cell-growth monitoring, and the rest of the sample was centrifuged for 10 min at 13,000 rpm (Micro-12; Hanil Scientific Co., Korea). The supernatants of the samples were stored at −40°C until further analysis.

Analysis of the Culture Products

The product (lactic acid) concentrations and carbon source concentrations were monitored with a high-performance liquid chromatography system (UV730D detector, RI750F monitor; Younglin, Korea). An ion-exchange column (Aminex HPX-87H, 300 mm×7.8 mm; BioRad, USA) was used with 0.01 N H_2SO_4 as the mobile phase at 50°C and a flow rate of 0.6 ml/min. Samples were transferred into a vial with filtration (13 mm, 0.2 μm PVDF syringe filter; Whatman, UK).

Glucose Pulse and Rapid-Sampling Experiment

After the glucose-limited chemostat condition was established, the glucose pulse experiment was conducted. The glucose pulse solution was prepared to give a total 5 mM of pulse. The glucose pulse concentration was adopted from the literature [23]. Because the steady-state concentration of glucose in the bioreactor was far less than 5 mM (0.26±0.07 g/l), 5 mM was a satisfactory concentration for the pulse of the substrate.

To monitor the dynamics of cellular metabolism, a rapid sampling experiment was followed with a sampling device (Foxy 200 X-Y Fraction Collector; Teledyne Technologies Company, USA) connected to the fermenter with a periplastic pump and refrigerating bath (RW-2040G; Jeiotech, Korea). Five ml of pulsed culture broth samples was mixed with the same volume of quenching solution in the tube, which was precooled to −40°C. The quenching solution was adopted from Faijes *et al*. [4], which is 0.85% (w/v) ammonium carbonate in a methanol solution. During 300 s, 100 pulsed samples were attained. The quenched samples were centrifuged at −20°C (Supra 22K; Hanil Scientific Co., Korea). After centrifugation, cell pellets were snapped frozen in liquid nitrogen and stored at −80°C until further processing.

Metabolite Extraction and LC–MS/MS Analysis

A modified cold methanol extraction method [4] was used for the intracellular metabolite extraction. First, cell pellets were suspended in 0.25 ml of −80°C absolute methanol. Second, suspended cell pellets were frozen in liquid nitrogen and thawed at −80°C. After the three freeze-thaw cycles were completed, samples were centrifuged at −10°C for 5 min at 13,000 rpm. The supernatants were stored at −80°C, and another 0.25 ml of cold methanol was added to the cell pellet. The same extraction cycle was conducted with the cell pellet, and supernatants were combined with the first one for a total volume of 0.5 ml.

The detection and quantification of intracellular metabolites were conducted with an HPLC system (Agilent 1200 series; Agilent Technologies, USA) coupled with an MS/MS system (API 3200 triple quadrupole mass spectrometer with turbo-ion spray source; AB/MDS Sciex, Canada). The Analyst software (version 1.4.2; AB/MDS Sciex, Canada) was used for the data manipulation. The operation condition of the mass spectrometer was as follows: negative ion and the selected reaction monitoring (SRM) mode. The parameters of declustering potential (DP), collision energy (CE), and collision cell exit potential (CXP) were optimized before the analysis. The entrance potential (EP) was fixed at −10 V, and the MS parameters were applied as follows: the ion spray voltage was set to −4,500 V, the nebulizer gas (GS1) and the auxiliary gas (GS2) were set to 20, the curtain gas (CUR) and the collision gas (CAD) were 10 and 5, respectively, and the GS2 temperature was set to be a constant value of 500°C. Synergi Hydro-RP (C18) 150 mm×2.1 mm I.D., 4 μm 80 Å particle columns (Phenomenex, USA) were used in the HPLC system at room temperature. Eluents A and B were 10 mM tributylamine aqueous solutions with their pH adjusted to 4.95 using 15 mM acetic acid and methanol, respectively. A binary gradient at a flow rate of 0.2 ml/min was applied using an HPLC pump. The intracellular metabolite quantification method was adopted from Luo *et al.* [13].

Metabolic Pathway Modeling

The metabolic pathway of *Lactococcus lactis* subsp. *lactis* (ATCC 19435) is depicted in Fig. 1. This metabolic model contains two glucose transfer systems: the hexose transporter (PERM) and phosphotransferase system (PTS). Most studies consider only one of the two systems or describe one as single flux *via* lumping [7, 8, 14, 21]. Although most of the lactic acid-producing bacteria use the PTS

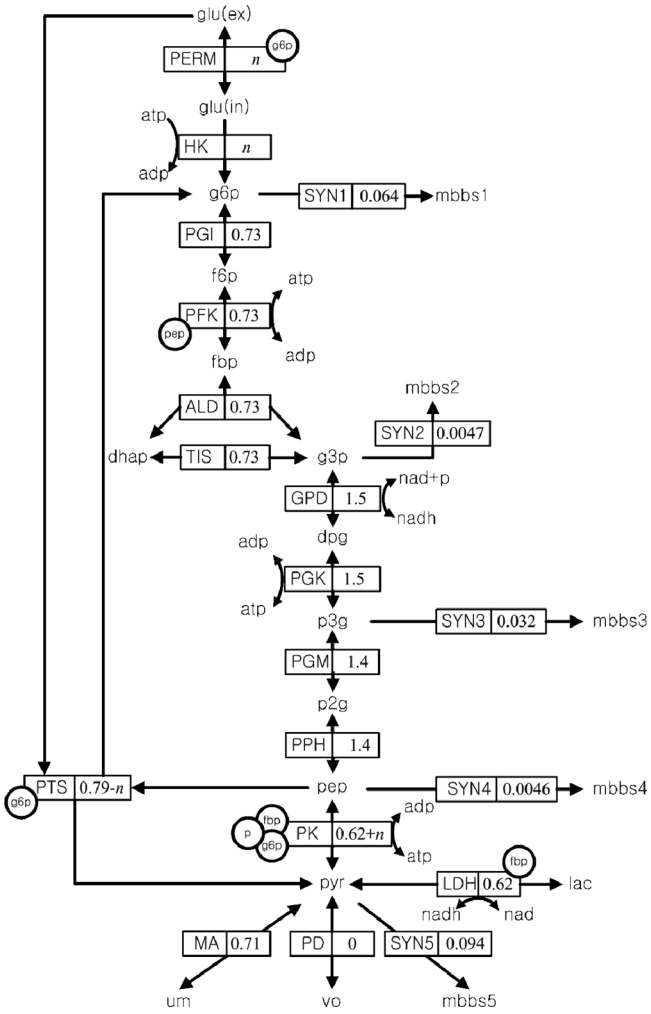

Fig. 1. Metabolic pathway of *Lactococcus lactis* subsp. *lactis* (ATCC 19435).
Uppercase letters, enzymes; circled letters, inhibitors; boxes, metabolic fluxes; arrows, metabolic flux directions.

system as a major glucose transport system [16], the PERM system is also activated as an alternative pathway [15, 16] and has to be considered as a transport system.

During the model construction process, the pentose phosphate pathway (PPP) system, the citrate cycle (TCA cycle), and some pathways of pyruvate metabolism are lumped as several individual fluxes (SYN1, SYN2, SYN3, SYN4, SYN5, PD, MA).

Previous research considered only the main streams of metabolic fluxes and did not consider biomass synthesis pathways or lump all synthesis pathways into a single flux [11, 14]. However, this model considers the detailed fluxes of biosynthesis (SYN1~5). This makes this model more reasonable than the other previously constructed models. Moreover, the flux distributions of these metabolisms can be calculated through a few assumptions: the pathways related to the PPP system are considered as the synthesis of macromolecules, such as nucleotides, proteins, lipids, and amino acids; all of these metabolites are precursors.

With these assumptions, the fluxes of these pathways are calculated through the macromolecular composition rate of biomass (g/g cell dry weight, SYN1~5).

Lactococcus lactis subsp. *lactis* (ATCC 19435) is reported as a homofermentative bacteria in glucose-rich conditions and also shows a heterofermentative character in certain situations [11, 16]. However, because all of the fermentation experiments were conducted in the homolactic fermentation condition, every pathway related to mixed acids or ethanol is lumped into the pyruvate dehydrogenase (PD) metabolism as various organic acids (vo). Unknown metabolites (um) are inserted as side branches of pyruvate metabolism to buffer the possible metabolic imbalances. (All of the used abbreviations are listed in the Nomenclature section) Each enzyme has its own reaction numbers for the convenience of further calculations.

Kinetic Rate Equations

The kinetic reaction rate equations for each enzyme were adopted from various studies, mainly Hoefnagel *et al.* [7] and Rizzi *et al.* [20]. These equations and initial values are shown in Tables 2 and 3.

For permease (PERM), the equation suggested by Rizzi *et al.* [19] was used. Although this equation was developed from the *Saccharomyces cerevisiae* strain, it is adopted as a generalized form of the equation for permease. The next step, hexokinase, is activated with the conversion of ATP into ADP (see Fromm and Zewe [5]). The reaction step of phosphoglucose isomerase (PGI) is set to be a reversible reaction because of the equilibrium assumption of this equation suggested by Richter *et al.* [18]. In phosphofructokinase (PFK), which is adopted from Hoefnagel *et al.* [8], pep acts as an inhibitor of this step, and ATP is dephosphorylated similarly to PGI, except that this step is reversible.

The sequential equation steps, which started from glyceraldehyde 3-phosphate to phosphoenolpyruvate (GPD, PGK, PGM, PPH), are adopted from Hoefnagel *et al.* [8], as well as the pyruvate kinase (PK) and lactate dehydrogenase (LDH). In the kinetic rate equation of the phosphotransferase system (PTS) adopted from Chassagnole *et al.* [1], there is the inhibition term of g6p. The generalized forms of the enzyme kinetic rate equations, such as the Michaelis–Menten equation (used in PD), and the reversible Michaelis–Menten equation (used in MA) or empirical equations (used in SYN1~5), are used in the lumped pathway.

Parameter Estimation and Metabolic Control Analysis (MCA)

Based on the measured intracellular metabolite concentration data and the time-course simulation result, the estimation of kinetic parameters and MCA were performed with the COPASI software (http://www.copasi.org). Because all of the metabolites in the pathway cannot be detected, the unmeasured metabolite concentrations were attained from the time-course simulation result. An evolutionary programming method was used for fitting the experimental data and kinetic parameters. The MCA was conducted with steady-state condition values and estimated parameters to verify the interactions between enzymes and metabolites.

RESULTS AND DISCUSSION

Metabolic Flux Analysis (MFA)

Based on the metabolic pathway of *Lactococcus lactis* subsp. *lactis* (ATCC 19435) as illustrated in Fig. 1, 11 mass balance equations were attained. As rearranged in

matrix notation, the mass balance equations can be described to have the form of Eq. (1):

$$r=G^{T}v\cdots\cdots \quad (1)$$

To make this metabolic system determined, the assumption is made that all biomass syntheses occur only with the fluxes given in this model. With this assumption, all fluxes of monomeric building blocks can be attained through calculation.

In the chemostat condition, the final concentrations of the substrate (glucose), product (lactic acid), and cell dry weight were 0.26±0.07 g/l, 3.99±0.21 g/l, and 1.29±0.41 g/l, respectively. All calculations followed the methods described by Stephanopoulos *et al.* [22].

The composition ratio data were adopted from the literature, and the synthesis ratio for each flux was calculated from the stoichiometric balance equations of related metabolites [22]. The calculation results are depicted in Table 1. With the biomass synthesis rates, the reaction rates of the measured fluxes can be calculated using the equations given by Stephanopoulos *et al.* [22].

Because no other acids were detected during the fermentation except lactic acid, the reaction rate of various organic acids (r_{13}) was zero. We also consider two glucose transport systems; as a result, the glucose uptake rate should be expressed as the summation form of PTS (r_1) and PERM (r_{15}). The result is shown in Fig. 1.

Table 1. Macromolecular synthesis rate for each flux.

Unit g/g CDW	SYN1	SYN2	SYN3	SYN4	SYN5	Sum[a]
Protein	0.024	-	0.090	0.023	0.38	0.52
RNA	0.080	-	0.043	-	0.037	0.16
DNA	0.015	-	0.0075	-	0.0075	0.030
Carbohydrate	0.17	-	-	-	-	0.17
Ash	0.030	-	-	-	-	0.030
Lipid	-	0.023625	0.021	-	0.045	0.090
Total	0.32	0.024	0.16	0.023	0.47	

Each column shows the macromolecular synthesis ratio for the selected pathway (added in the table).
[a]Sum of the proportions accounted for by each macromolecule in the cell dry weight. For example, there are 0.52 g/g CDW of protein in the cell biomass.

The flux analysis result shows a reasonable value that sufficiently supports the experimental result. The result shows that the fluxes through the other pathways are relatively small, except r_{14}. The flux to unknown metabolites was extremely large (0.71), almost the same as the glucose uptake flux (total 0.79). This can be explained by several reasons. First, the unconsidered biosynthesis fluxes appeared as unknown fluxes. Although every macromolecule was considered and calculated based on the composition ratio, it is possible that unconsidered molecules exist, such as sRNA. Second, fluxes to the TCA cycle may explain the unknown flux. Because the TCA cycle fluxes are not considered and are lumped as two fluxes (PD, SYN5), the

Table 2. Kinetic rate equations and parameters adopted in this study (equations taken from references are not given).

Enzyme	Kinetic rate equations	Parameter values
PD	$r_{PD}=r_{PD}^{max}\dfrac{C_{pyr}^{nPDH}}{K_{PD,pyr}+C_{pyr}^{nPDH}}$	r_{PD}^{max}=1.65 $K_{PD,pyr}$=1159 nPDH=3.68
MA	$r_{MA}=\dfrac{\dfrac{r_{pyr}^{max}C_{pyr}}{K_{MA,pyr}}-\dfrac{r_{um}^{max}C_{um}}{K_{MA,um}}}{1+\dfrac{C_{pyr}}{K_{MA,pyr}}+\dfrac{C_{um}}{K_{MA,um}}}2.0$	r_{pyr}^{max}=20 (random) r_{um}^{max}=5 (random) $K_{MA,pyr}$=3 (random) $K_{MA,um}$=6 (random)
SYN1	$r_{SYN1}=r_{SYN1}^{max}\dfrac{C_{g6p}}{K_{SYN1,g6p}+C_{g6p}}\dfrac{C_{atp}}{K_{SYN1,atp}+C_{atp}}$	r_{SYN1}^{max}=0.19 $K_{SYN1,g6p}$=2.7 $K_{SYN1,atp}$=0.4
SYN3	$r_{SYN3}=r_{SYN3}^{max}\dfrac{C_{p3g}}{K_{SYN3,p3g,14}+C_{p3g}}\dfrac{C_{atp}}{K_{SYN3,atp,14}+C_{atp}}$	r_{SYN3}^{max}=2 (random) $K_{SYN3,p3g}$=1.5 (random) $K_{SYN3,atp}$=0.2 (random)
SYN4	$r_{SYN4}=r_{SYN4}^{max}\dfrac{C_{pep}}{K_{SYN4,pep}+C_{pep}}\dfrac{C_{atp}}{K_{SYN4,atp}+C_{atp}}$	r_{SYN4}^{max}=1 (random) $K_{SYN4,pep}$=3 (random) $K_{SYN4,atp}$=8 (random)
SYN5	$r_{SYN5}=r_{SYN5}^{max}\dfrac{C_{pyr}}{K_{SYN5,pyr}+C_{pyr}}\dfrac{C_{atp}}{K_{SYN5,atp}+C_{atp}}$	r_{SYN5}^{max}=1.51 $K_{SYN5,pyr}$=0.92 $K_{SYN5,atp}$=13.2
SYN2	$r_{SYN2}=r_{SYN2}^{max}\dfrac{C_{g3p}}{K_{SYN2,g3p}+C_{g3p}}\dfrac{C_{atp}}{K_{SYN2,atp}+C_{atp}}$	r_{SYN2}^{max}=2 (random) $K_{SYN2,g3p}$=2 (random) $K_{SYN2,atp}$=6 (random)

Table 3. Initial concentrations used in the metabolic modeling with COPASI.

Metabolites	Initial concentration (mM)	Reference
glu(in)	0.00001	Empirical value
glu(ex)	1.443161634	Measured
g6p	3	[10]
f6p	0.7	[10]
fbp	0.0008	Measured
dhap	11	[10]
g3p	0.1	Measured
pep	0.00067	Measured
dpg	0.1	[10]
p	5	[10]
p3g	20	[10]
p2g	1.8	[10]
lac	0.1	[10]
mbbs1	3.21	Calculated
mbbs2	0.24	Calculated
mbbs3	1.63	Calculated
mbbs4	0.23	Calculated
mbbs5	4.75	Calculated
pyr	4.16×10^{-5}	Measured
atp	5	[10]
adp	5	[10]
amp	0.11	[10]
nad	5.2	[10]
nadh	0.35	[10]

rest of the TCA cycle fluxes are summed and illustrated as unknown metabolites. Third, fluxes to the synthesis of cometabolites may appear. Numerous co-metabolites exist in cell metabolism, such as adenosine phosphate groups, NADH, and NADPH. Metabolic fluxes related to these metabolites were not considered in this model. Although the metabolic fluxes of each of these metabolites might be insignificant, because there are various cometabolites, the sums of all these fluxes could be significant. Fourth, all listed reasons could have occurred at the same time.

Intracellular Metabolite Measurement in the Pulsed Sample

The intracellular metabolites of glucose-pulsed *Lactococcus lactis* subsp. *lactis* (ATCC 19435) were measured. The measured metabolites were fbp, g3p, pep, and pyr. The results are depicted on Fig. 2. At time zero, a 5 mM glucose pulse was given to the pool. All of the measured metabolites showed a rapid increase in concentration right after the pulse. The fbp concentration continuously increased during the 30 s. The g3p also increased rapidly, and at 15 s after the pulse, it reached its peak and rapidly decreased and reached a steady-state value that was much higher than the initial value. A fluctuation reaction appeared in the pep concentration. Although this fluctuation did not reach its steady-state value during the sampling time, a general decreasing pattern was observed. The pyr concentration reached its steady-state concentration most rapidly, only three seconds after the pulse, and showed a generally decreasing pattern as time went by. Although all of the measured metabolites showed their own characteristic reaction, the absolute concentration values were very different. The g3p showed 200-fold higher values compared with pyr and about 20-old higher than the others.

In the analysis of intracellular metabolites, g6p and f6p could not be detected. There are several explanations for this result. The most reasonable explanation is the conversion rate of the glycolysis pathway. Because glycolysis is the fastest pathways in almost every microorganism [2], during the sampling procedure these head metabolites of glycolysis could be degraded to the next metabolites. Moreover, because of their molecular similarity, metabolites between g3p to pep cannot be distinguished by mass spectrometry. These limited conditions caused large deviations in the parameter estimation. Although only the limited metabolites were identified, the tendencies of detected metabolites were quite similar to previous studies. Thompson [24] and Ramos *et al*. [17] reported this during the glycolysis process on fbp accumulation. The experiment of this study shows exactly the same pattern. For the attainment of a precise metabolic model, an accurate intracellular detection method should be established further.

Parameter Estimation

Parameters throughout the whole metabolic pathway were estimated using the COPASI software. Because there are limited data for the parameters to fit, the deviations are quite large (data not shown). However, through comparison of the MCA results between the estimated parameters and the original parameters, a more comprehensive understanding of the metabolic system can be achieved.

Metabolic Control Analysis

Prior to the sensitivity analysis, the condition number $C(G^T)$ of the stoichiometric matrix was measured. The result showed that this matrix had a condition number of 5.5, which implies that this system fulfilled the criteria of a well-conditioned matrix given by Stephanopoulos *et al.* [22].

As a result of MCA, the enzyme elasticity coefficients (ECC), flux control coefficients (FCC), and concentration control coefficients (CCC) were derived. To enhance the understanding of these results, the coefficients of the enzymes (reaction rates) related to lactic acid (target product), such as LDH, PK and PTS, are shown in Tables 4 to 6.

The elasticity coefficients with the original values show that LDH is positively affected the most by pyr. Then fbp is next to pyr in stimulating the reaction rate of LDH. Pyr also shows an inhibition effect on the PK reaction rate.

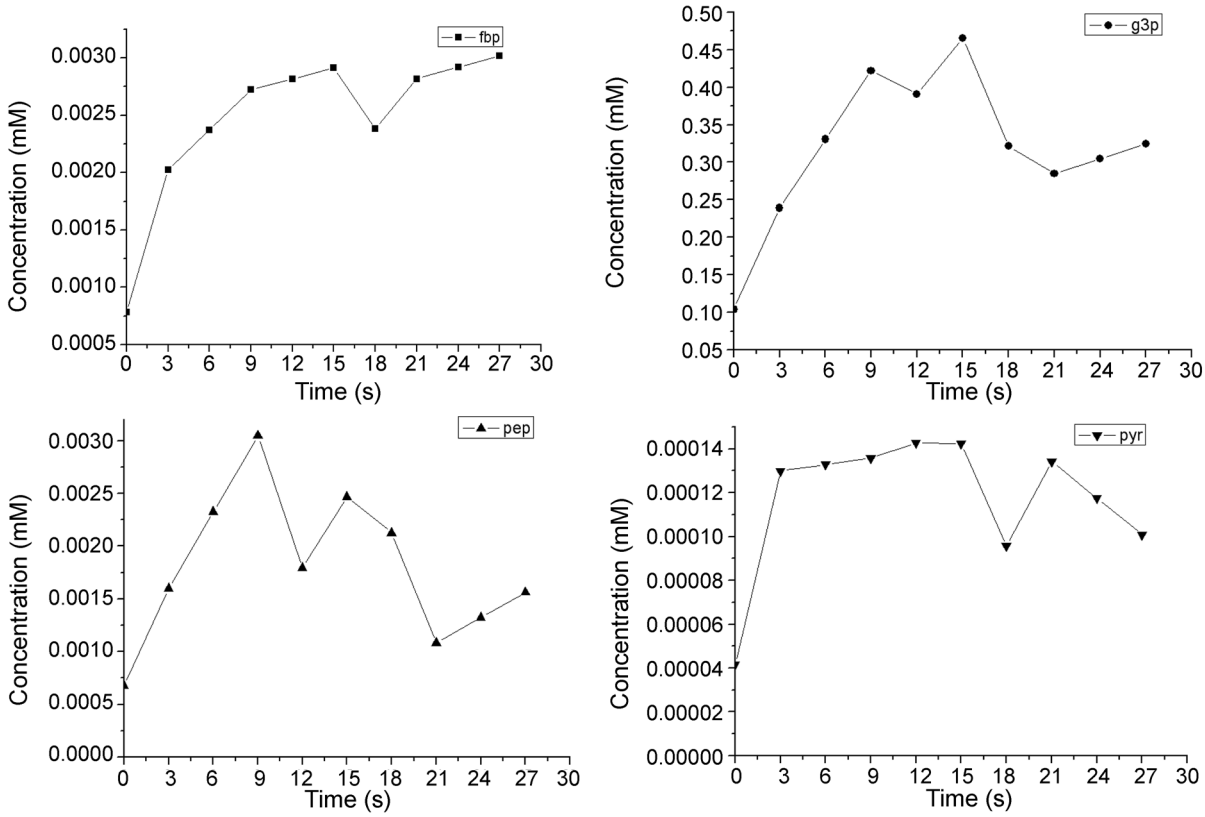

Fig. 2. Intracellular metabolite measurement data.
Samples were taken every 3 s from a glucose-pulsed chemostat condition fermentor. Subsequently, the samples were analyzed and quantified with an LC–MS/MS system.

G6p is the most efficient stimulator of PK. Additionally, pep is another good stimulator of PK aside from g6p. PTS is mostly inhibited by pyr, similar to PK. G6p acts as an inhibitor to PTS. Only pep stimulates the reaction rate of PTS. The elasticity coefficients with the estimated parameters show similar results with the original values, although their magnitudes are different. The difference was only significant for pep. With the estimated parameters, pep shows an inhibition effect on PK.

Table 4. Elasticity coefficients.

Reaction rate		Metabolite			
		pyr	g6p	pep	fbp
Original value	LDH	1	-	-	0.014
	PK	-1.4×10^{-4}	1.6	1.4	0.028
	PTS	-1	-0.29	1	-
Estimated value	LDH	0.000347	-	-	0.000286
	PK	-0.00181	0.036179	-0.00495	0.14449
	PTS	-	-	-	-

The original values show MCA results with the parameters in the references, and the estimated values show the MCA results with the parameters that were estimated in this paper.

The flux through LDH is mostly affected by PERM, and PERM also affects the metabolic flux of PK. However, PERM did not significantly affect PTS. The activity of PGI mostly affects the flux of PTS.

Because of the steady-state condition, all start-point metabolites and end-product metabolites are set to be constant values and are input as fixed values in the simulation software. Therefore, the CCC of pyr, right before lactate, was concerned as a main coefficient. The enzyme activity suggests that PERM has the greatest effect on pyr. Additionally, PGI shows a large value of CCC on pyr, next to PERM. Pep, the preceding step of pyr, is shown as being mostly sensitive to PGI and PFK, and the

Table 5. Flux control coefficients.

Flux (enzyme)	Enzyme					
	PERM	HK	PGI	PFK	ALD	PK
LDH	0.38	0.12	0.23	0.041	0.0031	-0.12
PK	0.53	0.17	0.19	0.034	0.0023	-
PTS	-0.43	-0.14	0.57	0.01	0.011	-0.51

These values indicate the effects of the enzyme activities (column) on the steady-state flux through each enzyme (row).

Table 6. Concentration control coefficients.

Metabolite	Enzyme activity				
	PERM	HK	PGI	PFK	LDH
pyr	0.34	0.12	0.23	0.040	-0.83
pep	0.023	0.0073	0.66	0.66	-0.096
g3p	0.32	0.10	0.35	0.35	0.11
fbp	0.55	0.18	0.34	0.34	0.24
g6p	0.31	0.10	-0.47	-0.081	0.14

These values indicate the metabolite's concentration (row) sensitivity due to certain enzyme (column) activities.

concentration change of pep is mostly unsensitive to the activity of LDH.

The metabolic control analysis shows remarkable results. As the ECC indicates, the activation effect of fbp on LDH was reported previously [24]. However, pyr appears to have much larger ECC values on LDH. This indicates that the reaction rate of LDH is more affected by the pyr concentration change, and obviously pyr has much more regulatory effects on LDH. Additionally, pyr acts as the most powerful inhibitor of PK and PTS. Although these regulatory effects of pyr on important enzymes may not be significant in the *in vivo* metabolism owing to its low concentration, this result could be used as a key strategy for the gene modification or further metabolic engineering. Moreover g6p, along with pep, shows a strong activation effect on PK. Because PK is considered the main enzyme for homolactic fermentation [16, 24], this result is important for researchers who intend to redirect the metabolic flux of lactic acid production. Unexpectedly, the FCC results showed that flux through LDH was mostly affected by the activity of PERM. Normally, PERM is considered as an alternative glucose transporter to PTS in LAB [15, 16], and therefore the enzyme activity of PERM has not been considered seriously. Further experimental data are required to verify this flux control effect. If this result stands, one could improve the lactic acid production rate by blocking the PTS pathway and increasing PERM activity. Based on FCC, PERM shows a strong activation effect on PK also. There were several attempts to produce other useful materials (besides lactic acid) [7, 11], and consequently this can be a guideline toward pyruvate metabolism enhancement. The CCC showed similar results to the FCC. The concentration change of pyr is most sensitive to the activity change of PERM, and the pep concentration is most sensitive to the activity change of PGI.

To construct an accurate metabolic model and to deepen the understanding of *Lactococcus lactis* subsp. *lactis* (ATCC 19435), a substrate pulse experiment was conducted with chemostat steady-state conditioned *Lactococcus lactis*. With experimental data and published results, we were able to perform kinetic modeling and estimate the parameters. Additionally, the results of the MFA and MCA gave insight into metabolism and its regulation effect of *Lactococcus lactis*.

These results are an important step towards the construction of complete metabolic modeling the in laboratory. Additionally, these results give key information about gene modifications and suggest the most efficient metabolic engineering strategy.

In the following steps, more detailed pathways should be considered, such as the TCA cycle or PPP system. To give more reliability to the MCA results, they should next be experimentally confirmed. Additionally, more accurate and global detection methods of intracellular metabolites must be established, not only for the metabolic engineering, but also for the enlargement of the metabolomics area.

Acknowledgements

This work was supported by the Koean Systems Biology Research Project (20100002168) of the Ministry of Education, Science and Technology (MEST) through the National Research Foundation of Korea. W. Won would like to acknowledge the financial support from the Seoul Metropolitan Government.

Abbreviations

glu(ex)	glucose external
glu(in)	glucose internal
g6p	glucose 6-phosphate
f6p	fructose 6-phosphate
fbp	fructose 1,6-bisphosphate
dhap	dihydroxyacetone phosphate
g3p	glyceraldehyde 3-phosphate
dpg	2,3-biphosphate
p3g	3-phosphoglycerate
p2g	2-phosphoglycerate
pep	phosphoenolpyruvate
pyr	pyruvate
mbbs	monomeric building blocks
nad	NAD^+
nadh	reduced form of NAD^+, NADH
p	phosphate
lac	lactic acid
vo	various organics
um	unknown metabolites
PERM	hexose transporter
PTS	phosphotransferase system
HK	hexokinase
PGI	phosphoglucose isomerase
PFK	phosphofructokinase
ALD	fructose bisphosphate aldolase
TIS	triose phosphate isomerase
GPD	glyceraldehyde 3-phosphate dehydrogenase
PGK	phosphoglycerate kinase
PGM	phosphoglycerate mutase
PPH	phosphopyruvate hydratase
PK	pyruvate kinase
LDH	lactate dehydrogenase
SYN	synthesis of monomeric building blocks

PD	pyruvate dehydrogenase
MA	mass action

References

1. Chassagnole, C., N. Noisommit-Rizzi, J. W. Schmid, K. Mauch, and M. Reuss. 2002. Dynamic modeling of the central carbon metabolism of *Escherichia coli*. *Biotechnol. Bioeng.* **79:** 53–73.
2. de Koning, W. and K. van Dam. 1992. A method for the determination of changes of glycolytic metabolites in yeast on a subsecond time scale using extraction at neutral pH. *Anal. Biochem.* **204:** 118–123.
3. Doi, Y. 1990. *Microbial Polyesters*. VCH Publishers, NY, USA.
4. Faijes, M., A. E Mars, and E. J. Smid. 2007. Comparision of quenching and extraction methodologies for metabolome analysis of *Lactobacillus plantarum*. *Microb. Cell Fact.* **6:** 27.
5. Fromm, H. J. and V. Zewe. 1962. Kinetics studies of yeast hexokinase. *J. Biol. Chem.* **237:** 3027–3032.
6. Heinrich, R. and T. A. Rapoport. 1974. A linear steady state treatment of enzymatic chains: General properties, control and effector strength. *Eur. J. Biochem.* **42:** 89–95.
7. Hoefnagel, M. H. N., M. J. C. Starrenburg, D. E. Martens, J. Hugenholtz, M. Kleerebezem, I. Van Swam, R. Bongers, H. V. Westerhoff, and J. L. Snoep. 2002. Metabolic engineering of lactic acid bacteria, the combined approach: Kinetic modelling, metabolic control and experimental analysis. *Microbiology* **148:** 1003–1013.
8. Hoefnagel, M. H. N., A. van der Burgt, D. E. Martens, J. Hugenholtz, and J. L. Snoep. 2002. Time dependent responses of glycolytic intermediates in a detailed glycolytic model of *Lactococcus lactis* during glucose run-out experiments. *Mol. Biol. Rep.* **29:** 157–161.
9. Ishii, N., M. Robert, Y. Nakayama, A. Kanai, and M. Tomita. 2004. Toward large-scale modeling of the microbial cell for computer simulation. *J. Biotechnol.* **113:** 281–294.
10. Kacser, H. and J. A Burns. 1973. The control of flux. *Symp. Soc. Exp. Biol*. **27:** 65–104.
11. Katoh, T., D. Yuguchi, H. Yoshii, H. Shi, and K .Shimizu. 1999. Dynamics and modeling on fermentative production of poly (β-hydroxybutyric acid) from sugars *via* lactate by a mixed culture of *Lactobacillus delbrueckii* and *Alcaligenes eutrophus*. *J. Biotechnol.* **67:** 113–134.
12. Lee, S. Y., D. Y. Lee, and T. Y. Kim. 2005. Systems biotechnology for strain improvement. *Trends Biotechnol.* **23:** 349–358.
13. Luo, B., K. Groenke, R. Takors, C. Wandrey, and M. Oldiges. 2007. Simultaneous determination of multiple intracellular metabolites in glycolysis, pentose phosphate pahtway and tricarboxylic acid cycle by liquid chromatography–mass spectrometery. *J. Chromatogr. A* **1147:** 153–164.
14. Melchiorsen, C. R., N. B. Siemsen Jensen, B. Christensen, V. K. Jokumsen, and J. Villadsen. 2000. Dynamics of pyruvate metabolism in *Lactococcus lactis*. *Biotechnol. Bioeng.* **74:** 271–279.
15. Neves, A. R., A. Ramos, C. M. Nunes, M. Kleerebezem, J. Hugenholtz, M. W. de Vos, J. Almeida, and H. Santos. 1999. *In vivo* nuclear magnetic resonance studies of glycolytic kinetics in *Lactococcus lactis*. *Biotechnol, Bioeng.* **64:** 200–212.
16. Neves, A. R., W. A. Pool, J. Kok, O. P. Kuipers, and H. Santos. 2005. Overview on sugar metabolism and its control in *Lactococcus lactis* – The input from *in vivo* NMR. *FEMS Microbiol. Rev.* **29:** 531–554.
17. Ramos, A., A. R. Neves, and H. Santos. 2002. Metabolism of lactic acid bacteria studied by nuclear magnetic resonance. *Antonie Van Leeuwenhoek* **82:** 249–261.
18. Richter, O., A. Betz, and C. Giersch. 1975. The response of oscillating glycolysis to perturbations in the NADH/NAD system: A comparison between experiments and a computer model. *BioSystems* **7:** 137–146.
19. Rizzi, M., U. Theobald, E. Querfurth, T. Rohrhirsch, M. Baltes, and M. Reuss. 1996. *In vivo* investigations of glucose transport in *Saccharomyces cerevisiae*. *Biotechnol. Bioeng.* **49:** 316–327.
20. Rizzi, M., M. Baltes, U. Theobald, and M. Reuss. 1997. *In vivo* analysis of metabolic dynamics in *Saccharomyces cerevisiae*; II. Mathematical model. *Biotechnol. Bioeng.* **55:** 592–608.
21. Sjoberg, A., I. Persson, M. Quednau, and B. Hahn-Hagerdal. 1995. The influence of limiting and non-limiting growth conditions on glucose and maltose metabolism in *Lactococcus lactis* ssp. *lactis* strains. *Appl. Microbiol. Biotechnol.* **42:** 931–938.
22. Stephanopoulos, G. N., A. A. Aristidou, and J. Nielsen. 1998. *Metabolic Engineering*. Academic Press, San Diego, USA.
23. Theobald, U., W. Mailinger, M. Blates, M. Rizzi, and M. Reuss. 1997. *In vivo* analysis of metabolic dynamics in *Saccharomyces cerevisiae*: I. Experimental observations. *Biotechnol. Bioeng.* **55:** 305–316.
24. Thompson, J. 1987. Regulation of sugar transport and metabolism in lactic acid bacteria. *FEMS Microbiol. Lett.* **46:** 221–231.
25. van Niel, W. J., K. Hofvendahl, and B. Hahn-Hagerdal. 2002. Formation and conversion of oxygen metabolites by *Lactococcus lactis* subsp. *lactis* ATCC 19435 under different growth conditions. *Appl. Environ. Microbiol.* **68:** 4350–4356.
26. Vickory, B. T. 1985. *Lactic Acid*, pp. 761–776. Dic Pergamon, Toronto, Canada.